


## ORIGINAL ARTICLE

# RITA1 drives the growth of bladder cancer cells by recruiting TRIM25 to facilitate the proteasomal degradation of RBPJ

Huancheng Tang<sup>1,2</sup>  | Xiangdong Li<sup>1,2</sup> | Lijuan Jiang<sup>1,2</sup> | Zefu Liu<sup>1,2</sup> | Lei Chen<sup>1,2</sup> | Jiawei Chen<sup>1,2</sup> | Minhua Deng<sup>1,2</sup> | Fangjian Zhou<sup>1,2</sup> | Xianchong Zheng<sup>1,2</sup> | Zhuowei Liu<sup>1,2</sup>

<sup>1</sup>Department of Urology, Sun Yat-Sen University Cancer Center, Guangzhou, China

<sup>2</sup>State Key Laboratory of Oncology in South China, Collaborative Innovation Center for Cancer Medicine, Sun Yat-sen University Cancer Center, Guangzhou, China

## Correspondence

Xianchong Zheng and Zhuowei Liu, Department of Urology, Sun Yat-sen University Cancer Center, No. 651, Dongfeng Road East, Guangzhou 510060, China.

Emails: zhengxc@sysucc.org.cn (X.Z.); liuzhw@sysucc.org.cn (Z.L.)

## Funding information

National Natural Science Foundation of China, Grant/Award Number: 81772716, 82002666, 82073103 and 82103264

## Abstract

Bladder cancer (BC) is one of the most prevalent malignancies worldwide, but it lacks effective targeted therapy due to its elusive molecular mechanism. Therefore, it is important to further investigate the molecular mechanisms that mediate BC progression. By performing a tumor tissue-based gene microarray and shRNA library screening, we found that recombination signal binding protein for immunoglobulin kappa J region (RBPJ) interacting and tubulin associated 1 (RITA1) is crucial for the growth of BC cells. Moreover, RITA1 is aberrantly highly expressed in BC tissues and is also correlated with poor prognosis in patients with BC. Mechanistically, we determined that RITA1 recruits tripartite motif containing 25 (TRIM25) to ubiquitinate RBPJ to accelerate its degradation via proteasome, which leads to the transcriptional inhibition of Notch1 downstream targets. Our results suggest that aberrant high expression of RITA1 drives the growth of BC cells via the RITA1/TRIM25/RBPJ axis and RITA1 may serve as a promising therapeutic target for BC.

## KEYWORDS

bladder cancer, proliferation, RBPJ, RITA1, TRIM25

## 1 | INTRODUCTION

Bladder cancer (BC) is one of the most prevalent malignancies worldwide, with a continuous increase in morbidity over the past few decades. There are an estimated 170,000 deaths from BC worldwide annually. Moreover, nearly 20% of new BC cases are muscle-invasive BC (MIBC). Due to the lack of effective therapeutic strategies, the

5-year overall survival (OS) rate for patients with MIBC is approximately 50%, with a poor prognosis.<sup>1,2</sup> Therefore, there is an urgent need to determine the pathogenic mechanisms mediating the progression of BC in order to find potential therapeutic targets.

Transcriptome abnormalities are key internal factors driving the progression of BC; however, knowledge regarding BC transcription is limited. To screen the potential molecular biomarkers of BC, we

**Abbreviations:** ATCC, American Type Culture Collection; Baf-1, bafilomycin A1; BC, bladder cancer; CCK-8, cell-counting kit-8; CHX, cycloheximide; Co-IP, cointeracted immunoprecipitation; HES1, Hes family bHLH transcription factor 1; HEY, hairy/enhancer-of-split related with YRPW motif; IHC, immunohistochemistry; MIBC, muscle-invasive bladder cancer; MS, mass spectrometry; OS, overall survival; PTM, post-translational modification; qPCR, quantitative polymerase chain reaction; RBPJ, recombination signal binding protein for immunoglobulin kappa J region; RITA1, RBPJ interacting and tubulin associated 1; shRNA, short hairpin RNA; siRNA, short interfering RNA; TRIM25, tripartite motif containing 25.

Huancheng Tang, Xiangdong Li, and Lijuan Jiang contributed equally to this work.

This is an open access article under the terms of the [Creative Commons Attribution-NonCommercial-NoDerivs](https://creativecommons.org/licenses/by-nc-nd/4.0/) License, which permits use and distribution in any medium, provided the original work is properly cited, the use is non-commercial and no modifications or adaptations are made.

© 2022 The Authors. *Cancer Science* published by John Wiley & Sons Australia, Ltd on behalf of Japanese Cancer Association.

compared the transcription levels of genes between BC tissues and their paired normal tissues via gene microarray. To identify genes that are essential for the growth of BC cells, we performed a proliferation-based screening, with a short hairpin RNA (shRNA) library targeting the top 24 genes highlighted by the gene microarray analysis. Notably, we found that RBPJ interacting and tubulin associated 1 (RITA1) is crucial for the growth of BC cells. RITA1 is a highly conserved protein with no apparent homology to any other protein. Interestingly, it has been reported that RITA1 impedes Notch signaling by facilitating the nuclear export of RBPJ.<sup>3,4</sup> However, the role of Notch signaling is heterogeneous among different tumors, and it has the potential to play oncogenic or tumor-suppressive roles. Similarly, many studies have shown that RITA1 acts heterogeneously in different tumors, including anal malignancies, breast cancer, and hepatocarcinoma.<sup>5-7</sup> Therefore, it is possible that Notch signaling and RITA1 are regulated heterogeneously in different tumors. Based on the above observations, we speculated that RITA1 and Notch signaling may have a unique regulatory mechanism in BC.

In our study, we identified the oncogenic effect of RITA1 in BC through in vivo and in vitro experiments. We also investigated a novel mechanism of RITA1 in impeding Notch1 signaling by recruiting TRIM25 to ubiquitinate and degrade RBPJ. In summary, our results explain the oncogenic role of RITA1 in BC via Notch1 signaling, providing a possibility for the molecular mechanism of targeting Notch downstream genes.

## 2 | MATERIALS AND METHODS

### 2.1 | Immunohistochemistry

The main steps of the immunohistochemistry (IHC) experiment were performed according to previous studies.<sup>8</sup> The results were obtained by double-blind reading, with scoring performed by two experienced pathologists. The staining index was recorded as negative = 0, weak brown = 1, moderate brown = 2, or dark brown = 3. RITA1-positive cells were identified by looking at the sections, and a final positive score was obtained based on their percentage: <5%, 0; 6%–25%, 1; 26%–50%, 2; 51%–75%, 3; 76%–100%, 4; the final

immunoreactivity score was then derived from the product of the staining index and the positive area score; 0–4 was low expression and 6–12 was high expression. Anti-RITA1 (NBP2-38441, 1:50 dilution, Novus Biologicals), anti-NOTCH1 (20687-1-AP, 1:200 dilution, Proteintech), and anti-RBPJ (5313, 1:3000 dilution, Cell Signaling Technology) were used for IHC.

### 2.2 | Cell lines and cell cultures

The cell lines used in this study were purchased from the American Type Culture Collection (ATCC) and were used with 10% fetal bovine serum (Invitrogen). In our laboratory, all cell lines were passaged for <6 months. The cells were incubated in a 37°C incubator at 5% CO<sub>2</sub> and saturated humidity.

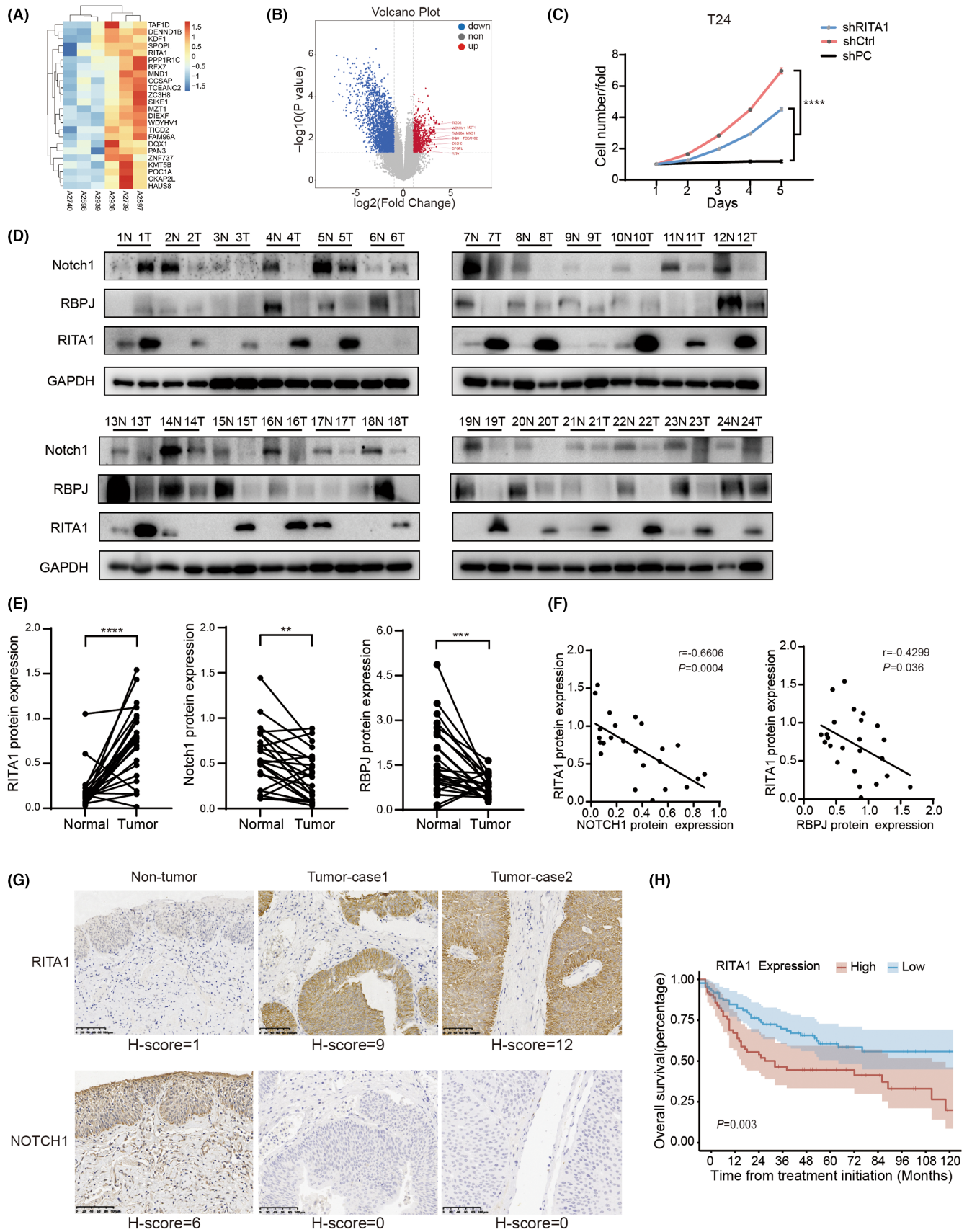
### 2.3 | Cell-counting kit-8 (CCK-8) assay

Transfected cells were seeded in 96-well plates for the corresponding time in an incubator. Subsequently, 10 μl of CCK reagent was added to each well and incubated according to the protocol of the CCK-8 assay kit (Dojindo). The absorbance of each well was measured at 450 nm using an enzyme-labeled instrument.

### 2.4 | Western blotting and cointeracted immunoprecipitation

Western blot was performed according to standard protocols. The intensities of bands were detected and quantified by ImageJ software. Nucleocytoplasmic protein fractionation was performed using an extraction kit for nuclear and cytoplasmic proteins (Beyotime) according to the manufacturer's protocol. For cointeracted immunoprecipitation (Co-IP), protein lysates were first incubated overnight at 4°C with anti-HA-magnetic beads, anti-Myc-magnetic beads, or anti-Flag-magnetic beads, and then the precipitates were washed three times with RIPA buffer and analyzed by protein blotting. The antibodies used in this experiment are shown in Table S2.

**FIGURE 1** RITA1 is overexpressed and negatively correlates with Notch1 expression in bladder cancer (BC), and its higher expression predicts poor prognosis in patients with BC. (A) Heatmap of two sets of bladder samples with expression profiles of representative differential genes, A2897, A2739, and A2938: tumor tissue; A2939, A2898, and A2740: normal tissue. (B) Volcano map of differentially expressed genes between tumor and normal bladder tissue. The representative genes that were significantly upregulated are identified in the graph. (C) Cell proliferation curves were plotted based on cell proliferation folds compared with the first day, with shPC as the positive target sequence. The data are plotted as the mean ± SD of three independent experiments. (D) The expressions of RITA1, RBPJ, and Notch1 proteins were examined by Western blot in 24 BC tissues and paired adjacent normal tissues. N, normal tissue; T, tumor tissue. GAPDH was assessed as an internal control. (E) The relative expression of RITA1 and Notch1, as well as RITA1 and RBPJ from (D) were quantified. (F) The correlation of the relative expressions of RITA1 and Notch1, as well as RITA1 and RBPJ were analyzed by Spearman's correlation analysis. (G) The expression of RITA1 and NOTCH1 was examined by immunohistochemistry (IHC) in BC tissues and adjacent normal bladder tissue. Scale bar, 100 μm. Representative images of evaluation of low expression (H-score ≤ 4) and high expression (H-score ≥ 6) staining are shown. (H) Kaplan-Meier analysis was used to predict the correlation between RITA1 expression and overall survival of 150 BC patients. \*\**p* < 0.01, \*\*\**p* < 0.001, \*\*\*\**p* < 0.0001



Variable	All cases (N = 150)	RITA1 expression (%)		p Value <sup>a</sup>
		Normal expression (N = 72)	Overexpression (N = 78)	
Age (years)				
≥60	83	38 (45.8%)	45 (54.2%)	0.545
<60	67	34 (50.8%)	33 (49.2%)	
Gender				
Female	18	9 (50%)	9 (50%)	0.856
Male	132	63 (47.8%)	69 (52.2%)	
Smoking history				
Yes	84	46 (54.8%)	38 (45.2%)	0.062
No	66	26 (39.4%)	40 (60.6%)	
Tumor size				
≥3 cm	53	18 (34.0%)	35 (66.0%)	0.006
<3 cm	97	54 (57.5%)	43 (42.5%)	
pT status				
T1	34	22 (64.7%)	12 (35.3%)	0.027
T2-T4	116	50 (43.1%)	66 (56.9%)	
pN status				
pN-	114	60 (52.6%)	54 (47.4%)	0.043
pN+	36	12 (33.3%)	24 (66.7%)	
Recurrence				
No	58	35 (60.3%)	23 (39.7%)	0.016
Yes	92	37 (40.2%)	55 (59.8%)	

<sup>a</sup>Chi-square test.

**TABLE 1** Correlation of RITA1 expression in tissue with patients' clinicopathological variables in 150 cases of BC

## 2.5 | RNA isolation and qRT-PCR analysis

In brief, total RNA from tissues and cells were extracted using TRIzol reagent (Invitrogen). The total RNA was synthesized into cDNA by using HiScript II Q RT SuperMix (Vazyme). Quantitative polymerase chain reaction (qPCR) was performed using SYBR Green Master Mix (Vazyme) on a Roche 480 quantitative real-time PCR system. The primers used to amplify the corresponding genes are displayed in Table S3.

## 2.6 | Statistical analysis

Data were analyzed using SPSS version 23.0 software (IBM Corp.). Survival curves were plotted by Kaplan-Meier analysis and compared by the log-rank test. Cox regression analysis was conducted to assess the significance of variables for survival. Data from cell line experiments are expressed as mean ± SD ( $X \pm SD$ ), and independent

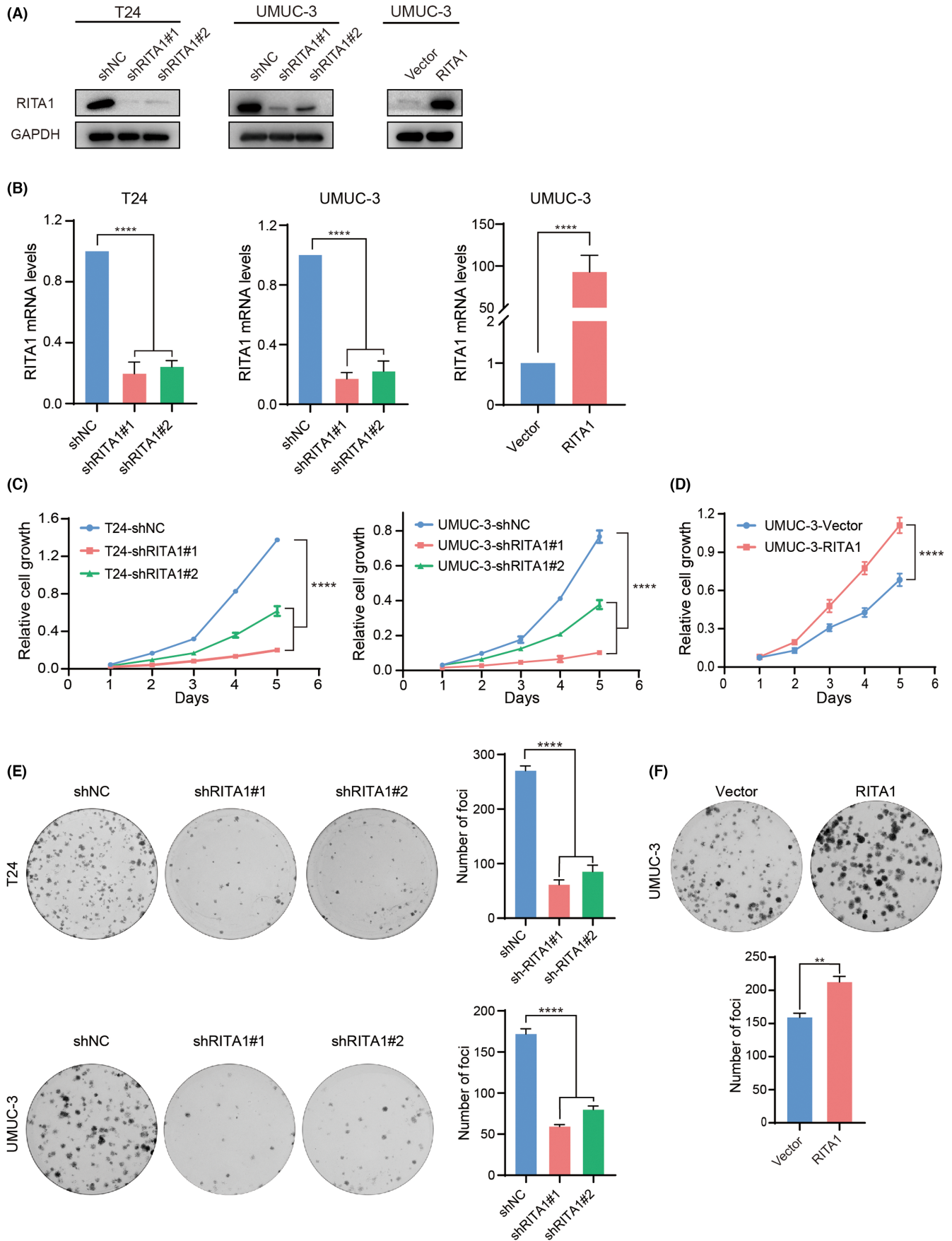
Student's *t* tests were used to analyze statistical significance between groups. *P* values <0.05 were considered statistically significant.

## 3 | RESULTS

### 3.1 | RITA1 is negatively correlated with Notch1 expression in BC, and its higher expression predicts poor prognosis in patients with BC

We compared the transcription levels of genes between BC tissues and their paired normal tissues via gene microarray. As a result, we identified 639 upregulated genes and 1473 downregulated genes in tumor tissues (supplementary excel file Table S5); the heatmap and volcano map are shown in Figure 1A,B. To identify genes that are essential for the growth of BC cells, we performed an shRNA library targeting the top 24 genes. Remarkably, we found that shRITA1 had a

**FIGURE 2** RITA1 promotes the growth of bladder cancer (BC) cells. (A) The stable-expression BC cells with RITA1 knockdown or overexpression were established by lentiviral infection. The expression of RITA1 protein in indicated stable expression cells was evaluated by Western blot. (B) The expression of RITA1 mRNA in indicated stable expression cells was assessed by qRT-PCR analysis. (C, D) The proliferation of indicated stable expression BC cells was evaluated by cell-counting kit-8 (CCK-8). The relative cell growth was analyzed. (E, F) The colony formation of the indicated stable expression BC cells was evaluated by colony formation assay. The number of colonies was calculated and analyzed. One-way ANOVA or Student's *t* test was applied to analyze and compare the data. The data are plotted as the mean ± SD of three independent experiments (B-F). \*\**p* < 0.01, \*\*\**p* < 0.001, \*\*\*\**p* < 0.0001



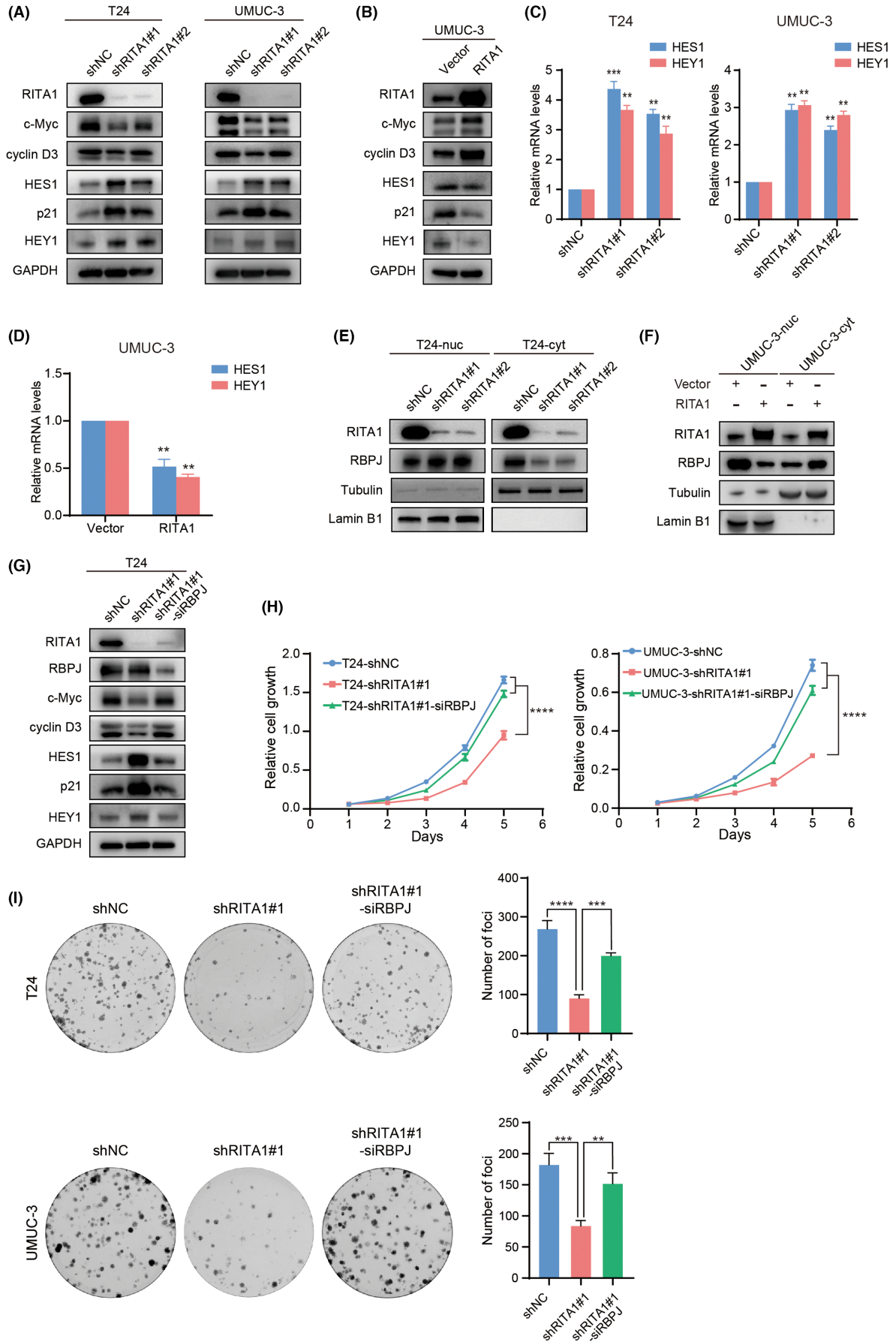


**FIGURE 3** RITA1 inhibits RBPJ-dependent Notch1 signaling in bladder cancer (BC) cells. (A, B) The protein expressions of Notch target genes in BC cells with RITA1 knockdown or overexpression were evaluated by Western blot. (C, D) The mRNA expression levels of Notch target genes in BC cells with RITA1 knockdown or overexpression were evaluated by qPCR. (E, F) The expression levels of RITA1 and RBPJ in nuclei and cytoplasm were analyzed by Western blot. Lamin B1 and tubulin were assessed as the internal control of nuclei and cytoplasm, respectively. (G) The expressions of Notch target genes in RITA1-knockdown T24 cells with or without RBPJ overexpression were evaluated by Western blot. (H, I) The proliferation and colony formation of RITA1-knockdown T24 or UMUC-3 cells with or without RBPJ overexpression were assessed by CCK-8 and colony-formation assay, respectively. The data are plotted as the mean  $\pm$  SD of three independent experiments (C, D, H, and I). \*\* $p < 0.01$ , \*\*\* $p < 0.001$ , \*\*\*\* $p < 0.0001$

significant inhibitory effect on the growth of BC cells (Figure 1C and Figure S1). To determine whether RITA1 was associated with Notch1 signaling in BC, we evaluated the expression of RITA1, RBPJ, and Notch1 in BC tissues and their paired normal tissues by Western blot (Figure 1D). We next analyzed the expression of these proteins relative to GAPDH. The results showed that RITA1 expression was higher in BC tissues than in paired paraneoplastic tissues. In contrast, RBPJ and Notch1 expression in BC tissues was significantly lower than that in paired paraneoplastic tissues (Figure 1E). Remarkably, the expressions of RITA1 and Notch were negatively correlated in BC tissues (Figure 1F). The negative correlation of protein expression between RITA1 and NOTCH1 was consistent with the microarray data. In addition, the protein expression levels of RITA1 and RBPJ were also negatively correlated in BC tissues (Figure 1F). These data indicated that higher expression of RITA1 and lower expression of Notch1 are associated with BC and they are negatively correlated with each other in BC.

To determine the role of RITA1 in predicting the prognosis of patients with BC, we examined RITA1 protein levels in the other 150 BC tissues by IHC staining (Table 1). The results showed that RITA1 was highly expressed in 65 BC cases, whereas normal bladder tissues had inadequate or low levels of RITA1. In contrast, lower expression of NOTCH1 was found in BC tissues than in adjacent normal bladder tissues (Figure 1G). Based on IHC staining data from 150 patients with BC, Kaplan-Meier analysis confirmed that higher expression of RITA1 was associated with less OS (Figure 1H). These results showed that higher expression of RITA1 predicts poor prognosis in patients with BC.

### 3.2 | RITA1 promotes the growth, migration, and invasion of BC cells

To verify the oncogenic function of RITA1, we knocked down the expression of RITA1 in T24 and UMUC-3 cells with two independent shRNAs by lentivirus. We also overexpressed the

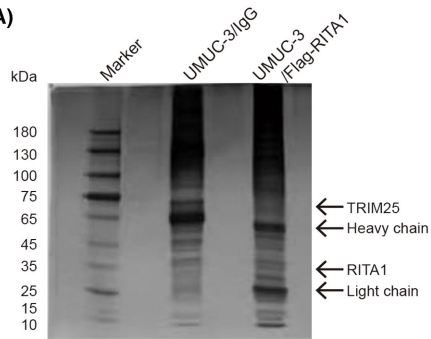
exogenous RITA1 in UMUC-3 cells. The expression of RITA1 in these stable-expression cells was validated by Western blot and qRT-PCR (Figure 2A,B). Next, we tested the proliferation of these stable-expression BC cells using a CCK-8 assay. Knockdown of RITA1 significantly inhibited, while overexpression of RITA1 significantly promoted the proliferation of BC cells (Figure 2C,D). We performed colony formation assay to validate this result. Similarly, knockdown of RITA1 reduced, while overexpression of RITA1 increased the number of colonies of BC cells (Figure 2E,F). Flow cytometry showed that knockdown of RITA1 significantly increased the percentage of apoptotic cells in both T24 and UMUC-3 cells (Figure S2). These results indicated that RITA1 promotes the growth of BC cells in vitro. In addition, we examined the role of RITA1 in BC cell migration and invasion using wound-healing assay and transwell invasion assay, respectively. Our data showed that knockdown of RITA1 suppressed the migration and invasion of BC cells, while overexpression of RITA1 promoted these properties (Figure S3).

### 3.3 | RITA1 inhibits Notch1 signaling to promote the growth of BC cells

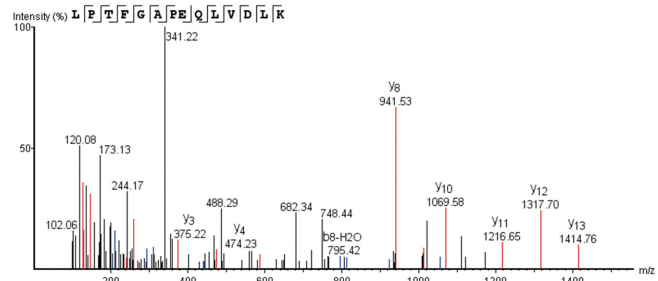
Previous studies have shown that RITA1 inhibits Notch signaling by interacting with RBPJ.<sup>3,9</sup> However, Notch signaling can be oncogenic or tumor suppressive in solid tumors, depending on the tissue type and tumor microenvironment. Therefore, we examined how RITA1 affects the expressions of Notch downstream targets by Western blot. We found that knockdown of RITA1 decreased the protein expression of c-Myc and cyclin D3 and increased the protein expression of Hes family bHLH transcription factor 1 (HES1), hairy/enhancer-of-split related with YRPW motif 1 (HEY1), and p21 in T24 and UMUC-3 cells (Figure 3A). Consistently, overexpression of RITA1 increased the protein expression of c-Myc and cyclin D3 but decreased the protein expression of HES1, HEY1, and p21 in UMUC-3 cells (Figure 3B). We

**FIGURE 4** RITA1 is required for the interaction of RBPJ and TRIM25 in UMUC-3 cells. (A) Immunoprecipitation (IP) was performed with IgG or Flag antibody of the lysate from Flag-RITA1-expressed UMUC-3 cells. The proteins in IP products were separated by SDS-PAGE and visualized by silver staining. The bands of TRIM25 and RITA1 are indicated by arrows. (B) The potential interacting proteins of RITA1 from the IP products were identified by mass spectrometry. The peptide segment diagram of TRIM25 is shown. (C) UMUC-3 cells were transfected with plasmids that express Myc-RITA1, Flag-RBPJ, and/or HA-TRIM25 in indicated combinations. The expressions of these exogenous proteins were validated by Western blot. (D–F) IP was performed with Myc, Flag, and HA antibodies using the cells mentioned in (C), and the expressions of Myc, Flag, and HA in the IP products were evaluated by Western blot. IgG were assessed as loading control. (G) IP was performed with Flag and HA antibodies between UMUC-3-shNC and UMUC-3-shRITA1#1. The expression of RITA1, Flag, and HA in the IP products were evaluated by Western blot

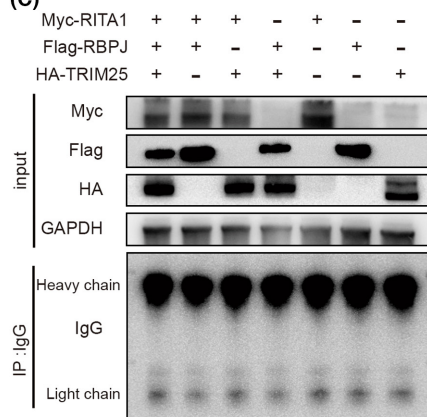
(A)



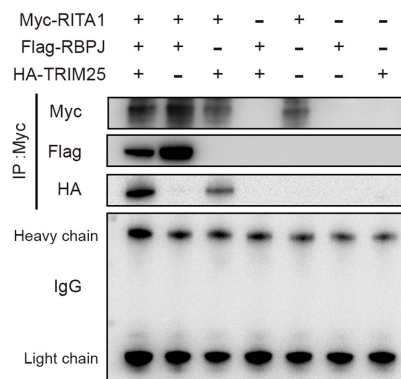
(B)



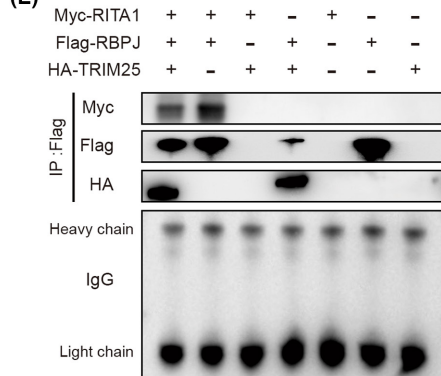
(C)



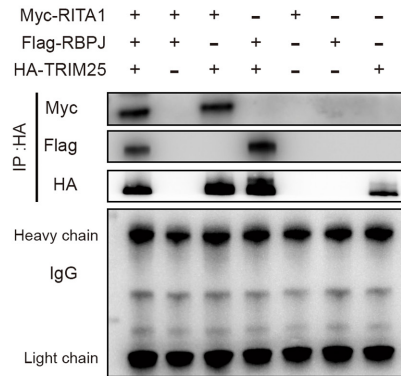
(D)



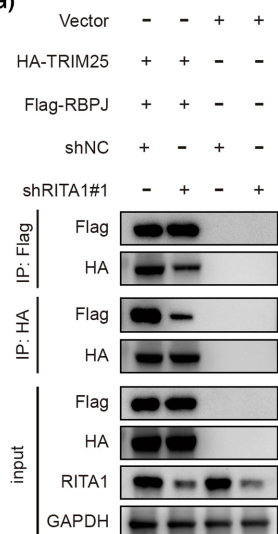
(E)



(F)



(G)





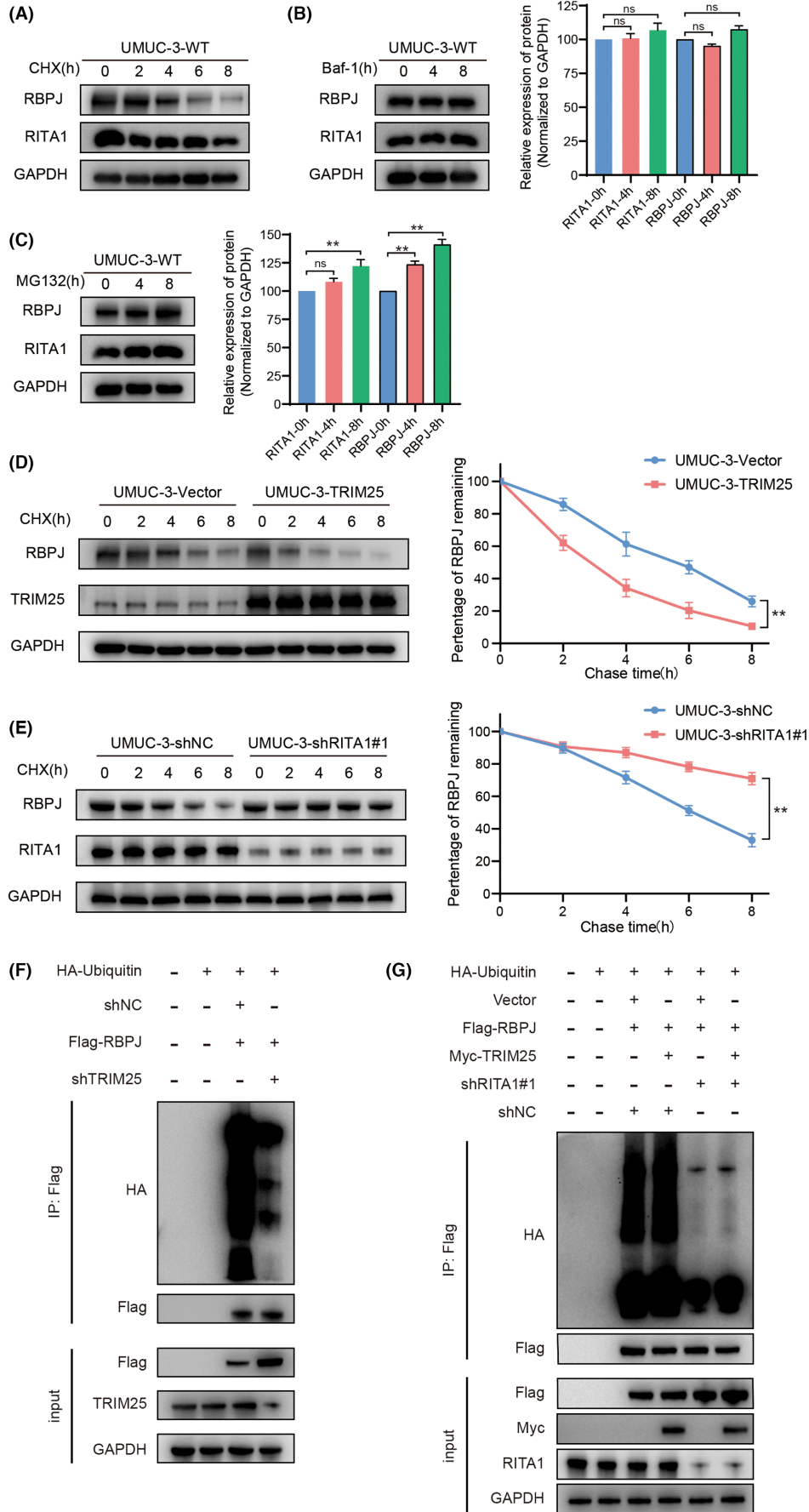


**FIGURE 5** TRIM25 ubiquitinates RBPJ in a RITA1-dependent manner. (A) UMUC-3 cells were treated with cycloheximide (CHX) for the indicated time. The expressions of RITA1 and RBPJ were detected by Western blot. (B, C) UMUC-3 cells were treated with Baf-1 and MG132 for the indicated time. The expressions of RITA1 and RBPJ were detected by Western blot. The densitometric analyses of the blots were performed from three independent experiments. (D, E) Different UMUC-3 stable cell lines were treated with 50  $\mu$ g/ml CHX for various durations, and the cell lysates were analyzed by Western blot. The densitometric analyses of the blots were performed from three independent experiments. The relative expressions of RBPJ in each group were quantified and presented as curve graph. (F, G) UMUC-3 cells with TRIM25 knockdown or Myc-TRIM25 expression, as well as RITA1 knockdown were transfected plasmids that express Flag-RBPJ and HA-ubiquitin. Cells were incubated with 10  $\mu$ M MG132 for 8 h prior to harvest. IP with Flag antibody, followed by Western blot analysis. ns, not significant; \* $p < 0.05$ , \*\* $p < 0.01$

found that knockdown of RITA1 increased the mRNA expression levels of HES1 and HEY1 in T24 and UMUC-3 cells. Consistently, RITA1 overexpression decreased the mRNA expression levels of HES1 and HEY1 in UMUC-3 cells (Figure 3C,D). We next analyzed whether RITA1 redistributed the levels of RBPJ, a transcriptional regulator important in the Notch signaling pathway, between the nucleus and cytoplasm. We found that knockdown of RITA1 increased the nuclear RBPJ and decreased the cytoplasmic RBPJ in T24 cells. Conversely, we found that overexpression of RITA1 resulted in increased cytoplasmic RBPJ and decreased nuclear RBPJ (Figure 3E,F).

As nuclear RBPJ directly governs Notch signaling and RITA1 inhibits Notch1 signaling, we next investigated whether RITA1 inhibited the Notch1 signaling through RBPJ. We used a specific siRNA to knock down RBPJ in RITA1-knocked-down T24 cells. Western blot analysis showed that knockdown of RBPJ in RITA1-knocked-down T24 cells restored the Notch1 signaling that was inhibited by RITA1 knockdown (Figure 3G). Moreover, data from the CCK-8 and colony formation assays showed that knockdown of RBPJ in RITA1-knocked-down T24 cells recovered the proliferation and colony formation that were suppressed by RITA1 knockdown (Figure 3H,I). Overall, these results indicated that RITA1 inhibits RBPJ-dependent Notch1 signal in BC cells.

### 3.4 | RITA1 recruits TRIM25 to interact with RBPJ in UMUC-3 cells

We next sought to explore the potential mechanism of RITA1 in orchestrating the subcellular distribution of RBPJ. To this end, we performed immunoprecipitation followed by mass spectrometry (MS) to identify the potential interacting proteins of RITA1 in UMUC3 cells. Surprisingly, we found that tripartite motif containing 25 (TRIM25), a E3 ubiquitin ligase, was identified in the interacting candidates of RITA1 (Figure 4A,B). Meanwhile, we noted that numerous 26S proteasome subunits were shown in the interaction list (Table S4).

As RBPJ is widely reported to interact with RITA1,<sup>3,9</sup> we speculated that RITA1 recruits TRIM25 to ubiquitinate RBPJ and promote its degradation by the proteasome. If this were true, RITA1, RBPJ, and TRIM25 would probably interact with each other and be located together. To investigate this, we cotransfected plasmids expressing these three proteins with different tags in UMUC-3 cells followed by immunoprecipitation. Data from Western blot

showed that RITA1, RBPJ, and TRIM25 interacted with each other in UMUC-3 cells (Figure 4C-F). Following knockdown of RITA1, the protein HA-TRIM25 was significantly reduced by the coimmunoprecipitation of Flag-RBPJ as a bait, and, similarly, the protein Flag-RBPJ was significantly reduced by using the coimmunoprecipitation of HA-TRIM25 as a bait (Figure 4G). Taken together, these results indicated that RITA1, RBPJ, and TRIM25 interacted with each other, and that RITA1 was required for the interaction of RBPJ and TRIM25.

### 3.5 | TRIM25 ubiquitinates RBPJ in a RITA1-dependent manner

Our data revealed that RBPJ could colocalize with RITA1 in the proteasome and also interact with TRIM25 in a RITA1-dependent manner. Therefore, we sought to identify whether RITA1 recruited TRIM25 to promote the proteasomal degradation of RBPJ. We inhibited protein synthesis with cycloheximide (CHX) to observe the stability of RBPJ and RITA1 in UMUC-3 cells. Data from Western blot showed that RBPJ, but not RITA1, was unstable in UMUC-3 cells (Figure 5A). Further, we treated UMUC-3 cells with lysosome inhibitor bafilomycin A1 (Baf-1) and proteasome inhibitor MG132 to determine the degradation pathway of RBPJ. Indeed, inhibition of the proteasome but not the lysosome obviously increased the stability of RBPJ in UMUC-3 cells (Figure 5B,C).

To determine whether TRIM25 accelerated the degradation of RBPJ in BC cells, we overexpressed TRIM25 in UMUC-3 cells followed by treatment with CHX. Data from Western blot and protein remaining curve showed that overexpression of TRIM25 decreased the half-life of RBPJ in UMUC-3 cells (Figure 5D). We also examined whether RITA1 had any effect on the half-life of RBPJ protein. In the presence of CHX, RBPJ appeared to become more stable after knocking down RITA1, suggesting a significant RITA1-dependent decline in RBPJ protein levels with a distinct reduction in half-life (Figure 5E). We performed a ubiquitination assay to confirm our observation. Western blot showed that knockdown of TRIM25 reduced the ubiquitination level of RBPJ in UMUC-3 cells (Figure 5F). Importantly, we observed that knockdown of RITA1 reduced the ubiquitination of RBPJ that was mediated by TRIM25 (Figure 5G). Overall, these results indicated that TRIM25 ubiquitinates RBPJ to promote its degradation by the proteasome in a RITA1-dependent manner.

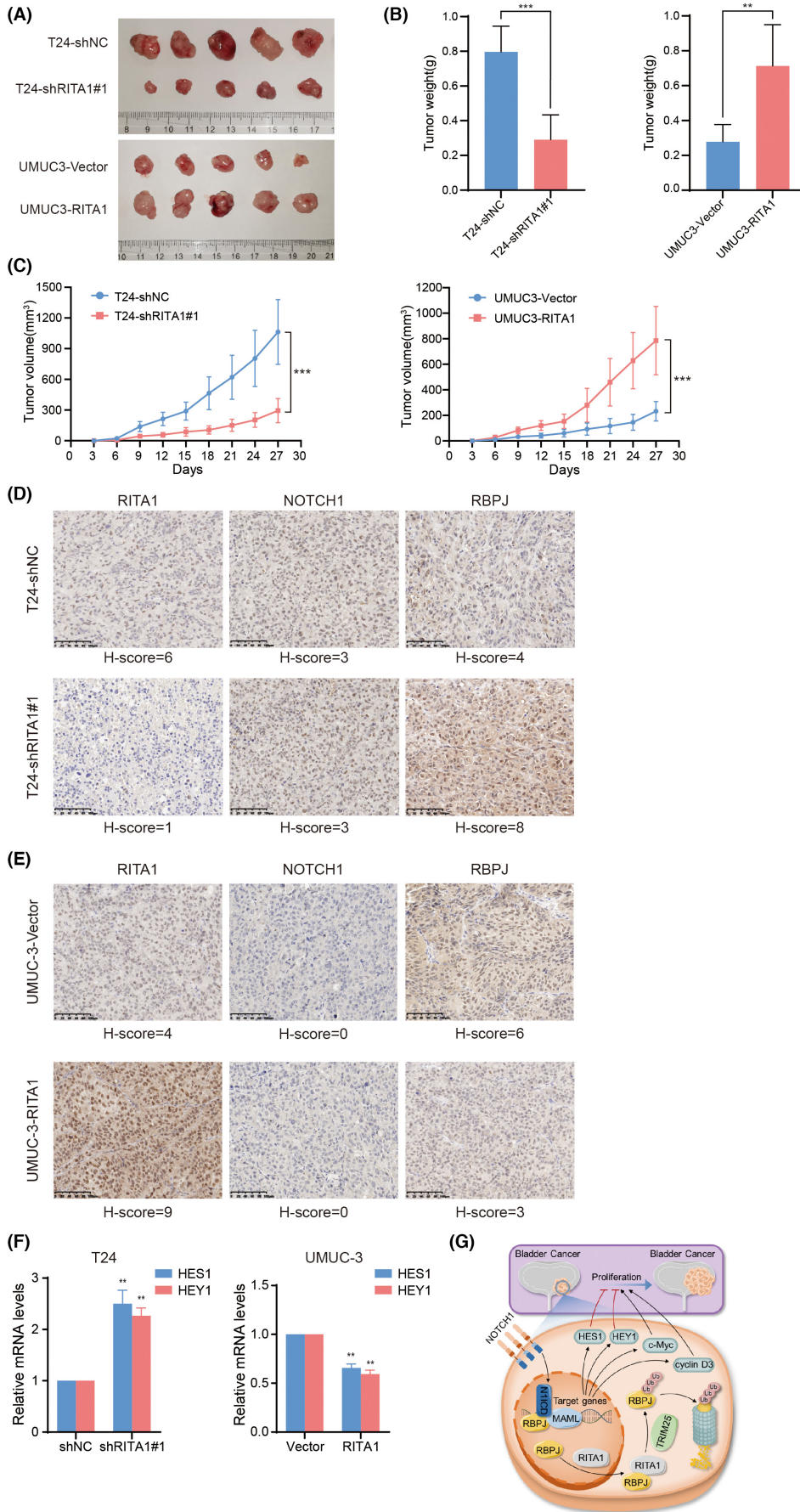


**FIGURE 6** RITA1 promotes the growth of bladder cancer (BC) cells in a mouse xenograft model. (A) The effect of RITA1 in tumor growth was determined in a nude mouse tumor xenograft model. The images of xenograft tumors from T24 cells with RITA1 knockdown or UMUC-3 cells with RITA1 overexpression ( $n = 5$  mice/group). (B) Tumor weights were analyzed. Data are expressed as the mean  $\pm$  SD.  $n = 5$  per group as indicated. (C) The tumor volumes at the indicated days were measured and analyzed. Data are expressed as the mean  $\pm$  SD.  $n = 5$  per group as indicated. Student's *t* test or two-way ANOVA was applied to analyze and compare the data. (D, E) We examined RITA1, NOTCH1, and RBPJ protein levels in different mice tumors by immunohistochemistry (IHC) staining. Scale bars, 100  $\mu$ m. Representative images of evaluation of low expression (H-score  $\leq 4$ ) and high expression (H-score  $\geq 6$ ) staining are shown. (F) The mRNA expressions of Notch target genes in different mice tumors with RITA1 knockdown or overexpression were evaluated by qPCR. The data are plotted as the mean  $\pm$  SD of three independent experiments. (G) The proposed model reveals that RITA1 recruits TRIM25 to ubiquitinate and degrade RBPJ, thus inhibiting Notch signaling to promote the growth of BC cells.  $**p < 0.01$ ,  $***p < 0.001$

### 3.6 | RITA1 promotes the growth of BC cells in a mouse xenograft model

Finally, to verify the effect of RITA1 on tumor growth in vivo, we used a subcutaneous tumor-forming xenograft nude mouse model. To generate this model, we subcutaneously inoculated T24 cells with RITA1 knockdown or UMUC-3 cells with RITA1 overexpression. Remarkably, knockdown of RITA1 in T24 cells suppressed the growth of tumors, as determined by reduced tumor size, weight, and volume (Figure 6A–C). In contrast, overexpression of RITA1 in UMUC-3 cells markedly promoted the growth of tumors (Figure 6A–C). We further analyzed the critical role of RITA1 in the mouse xenograft model. We found that the protein expression of RBPJ, but not NOTCH1, increased in xenografts derived from T24 cells with RITA1 knockdown; conversely, the protein expression of RBPJ, but not NOTCH1, decreased in xenografts derived from UMUC-3 cells with RITA1 overexpression (Figure 6D,E). We found that the mRNA expression levels of HES1 and HEY1 increased after the knockdown of RITA1, while the mRNA expression levels of HES1 and HEY1 decreased after overexpression of RITA1 (Figure 6F). These results indicated that RITA1 promotes the growth of BC cells in vivo, which verified the finding that RITA1 promotes the growth of BC cells in vitro.

## 4 | DISCUSSION

Notch signaling has been proven to play various roles in tumor progression, including tumor growth, invasion, metastasis, and even tumor immunity.<sup>10–12</sup> The role of Notch signaling is fairly heterogeneous among different tumors and has the potential to be oncogenic or tumor suppressive.<sup>13–20</sup> Although inactivation of Notch signaling is associated with BC progression, the regulatory mechanism of Notch downstream targets remains unclear.<sup>21–25</sup> In this study, we identified a novel mechanism whereby overexpression of RITA1 drives the growth of BC cells by recruiting TRIM25 to ubiquitinate RBPJ and accelerate its proteasomal degradation, thus leading to the transcriptional inhibition of Notch1 downstream targets (Figure 6G).

As a transcription factor, RBPJ is an integral component of Notch signaling, which activates the transcription of target genes, including those of the HES and HEY family.<sup>26</sup> It has been previously reported that RITA1 suppresses Notch signaling by facilitating the

nuclear export of RBPJ.<sup>3</sup> The excessive accumulation of RBPJ in the cytoplasm may also re-enter the nucleus and reactivate Notch signaling. As RITA1 can dramatically inhibit Notch signaling, we speculated that RITA1 may have further functions on RBPJ. Indeed, our molecular investigation demonstrated that RITA1 served as a bridge between RBPJ and TRIM25, which accelerates the proteasomal degradation of cytoplasmic RBPJ. Deshmukh et al.<sup>27</sup> have previously reported that cyclin F could mediate polyubiquitylation of RBPJ at Lys315. Therefore, we wondered whether there are other ways of ubiquitinating degradation of RBPJ. Intriguingly, RITA1 could also recruit RBPJ to the proteasome, providing a site for its degradation. Thus, our data suggested that inhibition of RBPJ-mediated Notch1 signaling by RITA1 is multifaceted.

Post-translational modification (PTM) has a direct regulatory effect on the activation or inactivation of protein functions.<sup>28</sup> In tumors, the PTM of proteins is relatively active, especially for key signal molecules that mediate tumor progression, which play a decisive role in the activation of oncogenes or the inactivation of tumor suppressors.<sup>29</sup> However, as a transcription factor regulating canonical Notch signaling, the PTM of RBPJ has rarely been reported. Although it was previously reported that RITA1 can facilitate the nuclear export of RBPJ,<sup>3</sup> its PTM is unknown. Through further investigation, we found that in BC cells, RITA1 is relatively stable, while RBPJ is easily degraded. It is easy to speculate that stable proteins may assist in the degradation of unstable proteins. Through RBPJ interaction-based MS, we found that TRIM25 is a potential E3 ligase of RBPJ. More importantly, we found that the ubiquitination and degradation of RBPJ are dependent on RITA1. We have reported for the first time that TRIM25 is the E3 ligase of RBPJ. Indeed, the oncogenic function of TRIM25 has also been reported in various tumors, including prostate cancer,<sup>30</sup> hepatocellular carcinoma,<sup>31</sup> and colorectal cancer.<sup>32</sup> We suspect that this is most likely to be related to the degradation of RBPJ and inhibition of the Notch1 signaling. Nevertheless, concrete evidence is necessary to clarify this matter, such as the ubiquitination site of RBPJ by TRIM25.

In conclusion, we demonstrate that aberrant upregulation of RITA1 is crucial for maintaining the growth of BC cells by inhibiting Notch1 signaling. We determined a novel mechanism whereby RITA1 recruits TRIM25 to ubiquitinate RBPJ to accelerate its proteasomal degradation, which leads to the transcriptional inhibition of Notch1 downstream targets. Therefore, the RITA1/TRIM25/RBPJ axis may serve as a therapeutic target for BC.

## ACKNOWLEDGMENT

This work was supported by grants from the National Natural Science Foundation of China (82073103 and 81772716 to Z.L., 82103264 to X.Z., and 82002666 to X.L.).

## DISCLOSURE

The authors declare no conflict of interest.

## ETHICS STATEMENT

Approval of the research protocol by an institutional reviewer board: This study was reviewed and approved by the Ethics Committee of Sun Yat-sen University Cancer Center (approval Nos.: B2019-227 and B2022-117).

## ANIMAL STUDIES

Animal experiments were performed in strict accordance with the "Guide for the Care and Use of Laboratory Animals" and were approved by the Animal Ethics Committee of Sun Yat-sen University Cancer Center (approval no.: L102042021040E).

## ORCID

Huancheng Tang  <https://orcid.org/0000-0002-3671-6073>

## REFERENCES

- Malkowicz SB, van Poppel H, Mickisch G, et al. Muscle-invasive urothelial carcinoma of the bladder. *Urology*. 2007;69:3-16. doi:10.1016/j.urology.2006.10.040
- Patel VG, Oh WK, Galsky MD. Treatment of muscle-invasive and advanced bladder cancer in 2020. *CA Cancer J Clin*. 2020;70:404-423. doi:10.3322/caac.21631
- Wacker SA, Alvarado C, von Wichert G, et al. RITA, a novel modulator of Notch signalling, acts via nuclear export of RBP-J. *EMBO J*. 2011;30:43-56. doi:10.1038/emboj.2010.289
- Wang H, Yang Z, Liu C, et al. RBP-J-interacting and tubulin-associated protein induces apoptosis and cell cycle arrest in human hepatocellular carcinoma by activating the p53-Fbxw7 pathway. *Biochem Biophys Res Commun*. 2014;454:71-77. doi:10.1016/j.bbrc.2014.10.023
- Wang H, Chen G, Wang H, Liu C. RITA inhibits growth of human hepatocellular carcinoma through induction of apoptosis. *Oncol Res*. 2012;20:437-445. doi:10.3727/096504013X13685487925059
- Hook SC, Ritter A, Steinhäuser K, et al. RITA modulates cell migration and invasion by affecting focal adhesion dynamics. *Mol Oncol*. 2019;13:2121-2141. doi:10.1002/1878-0261.12551
- Rödel F, Steinhäuser K, Kreis N, et al. Prognostic impact of RITA expression in patients with anal squamous cell carcinoma treated with chemoradiotherapy. *Radiother Oncol*. 2018;126:214-221. doi:10.1016/j.radonc.2017.10.028
- Li XD, Huang CW, Liu ZF, et al. Prognostic role of the immunoscore for patients with urothelial carcinoma of the bladder who underwent radical cystectomy. *Ann Surg Oncol*. 2019;26:4148-4156. doi:10.1245/s10434-019-07529-y
- Tabaja N, Yuan Z, Oswald F, Kovall RA. Structure-function analysis of RBP-J-interacting and tubulin-associated (RITA) reveals regions critical for repression of Notch target genes. *J Biol Chem*. 2017;292:10549-10563. doi:10.1074/jbc.M117.791707
- Artavanis-Tsakonas S, Rand MD, Lake RJ. Notch signaling: cell fate control and signal integration in development. *Science*. 1999;284:770-776. doi:10.1126/science.284.5415.770
- Wilson A, Radtke F. Multiple functions of Notch signaling in self-renewing organs and cancer. *FEBS Lett*. 2006;580:2860-2868. doi:10.1016/j.febslet.2006.03.024
- Wang J, Sullenger BA, Rich JN. Notch signaling in cancer stem cells. *Adv Exp Med Biol*. 2012;727:174-185. doi:10.1007/978-1-4614-0899-4\_13
- Reedijk M, Odorcic S, Chang L, et al. High-level coexpression of JAG1 and NOTCH1 is observed in human breast cancer and is associated with poor overall survival. *Cancer Res*. 2005;65:8530-8537. doi:10.1158/0008-5472.CAN-05-1069
- Fan X, Mikolaenko I, Elhassan I, et al. Notch1 and notch2 have opposite effects on embryonal brain tumor growth. *Cancer Res*. 2004;64:7787-7793. doi:10.1158/0008-5472.CAN-04-1446
- Nguyen BC, Lefort K, Mandinova A, et al. Cross-regulation between Notch and p63 in keratinocyte commitment to differentiation. *Genes Dev*. 2006;20:1028-1042. doi:10.1101/gad.1406006
- Viatour P, Ehmer U, Saddic LA, et al. Notch signaling inhibits hepatocellular carcinoma following inactivation of the RB pathway. *J Exp Med*. 2011;208:1963-1976. doi:10.1084/jem.20110198
- Baumgart A, Mazur PK, Anton M, et al. Opposing role of Notch1 and Notch2 in a KrasG12D-driven murine non-small cell lung cancer model. *Oncogene*. 2014;34:578-588. doi:10.1038/ncr.2013.592
- Hanlon L, Avila JL, Demarest RM, et al. Notch1 functions as a tumor suppressor in a model of K-ras-induced pancreatic ductal adenocarcinoma. *Cancer Res*. 2010;70:4280-4286. doi:10.1158/0008-5472.CAN-09-4645
- Mazur PK, Einwachter H, Lee M, et al. Notch2 is required for progression of pancreatic intraepithelial neoplasia and development of pancreatic ductal adenocarcinoma. *Proc Natl Acad Sci USA*. 2010;107:13438-13443. doi:10.1073/pnas.1002423107
- Hayashi T, Gust KM, Wyatt AW, et al. Not all NOTCH is created equal: the oncogenic role of NOTCH2 in bladder cancer and its implications for targeted therapy. *Clin Cancer Res*. 2016;22:2981-2992. doi:10.1158/1078-0432.CCR-15-2360
- Maraver A, Fernandez-Marcos PJ, Cash TP, et al. NOTCH pathway inactivation promotes bladder cancer progression. *J Clin Invest*. 2015;125:824-830. doi:10.1172/JCI78185
- Rampias T, Vgenopoulou P, Avgeris M, et al. A new tumor suppressor role for the Notch pathway in bladder cancer. *Nat Med*. 2014;20:1199-1205. doi:10.1038/nm.3678
- Schulz GB, Elezkurtaj S, Börding T, et al. Therapeutic and prognostic implications of NOTCH and MAPK signaling in bladder cancer. *Cancer Sci*. 2021;112:1987-1996. doi:10.1111/cas.14878
- Greife A, Jankowiak S, Steinbring J, et al. Canonical Notch signaling is inactive in urothelial carcinoma. *BMC Cancer*. 2014;14:628. doi:10.1186/1471-2407-14-628
- Yuan X, Wu H, Xu H, et al. Notch signaling: an emerging therapeutic target for cancer treatment. *Cancer Lett*. 2015;369:20-27. doi:10.1016/j.canlet.2015.07.048
- Guruharsha KG, Kankel MW, Artavanis-Tsakonas S. The Notch signalling system: recent insights into the complexity of a conserved pathway. *Nat Rev Genet*. 2012;13:654-666. doi:10.1038/nrg3272
- Deshmukh RS, Sharma S, Das S. Cyclin F-dependent degradation of RBPJ inhibits IDH1R132H-mediated tumorigenesis. *Cancer Res*. 2018;78:6386-6398. doi:10.1158/0008-5472.CAN-18-1772
- Qing G, Lu Q, Xiong Y, et al. New opportunities and challenges of smart polymers in post-translational modification proteomics. *Adv Mater*. 2017;29:1-18. doi:10.1002/adma.201604670
- Sun T, Liu Z, Yang Q. The role of ubiquitination and deubiquitination in cancer metabolism. *Mol Cancer*. 2020;19:146. doi:10.1186/s12943-020-01262-x
- Takayama KI, Suzuki T, Tanaka T, et al. TRIM25 enhances cell growth and cell survival by modulating p53 signals via interaction with G3BP2 in prostate cancer. *Oncogene*. 2018;37:2165-2180. doi:10.1038/s41388-017-0095-x

31. Liu Y, Tao S, Liao L, et al. TRIM25 promotes the cell survival and growth of hepatocellular carcinoma through targeting Keap1-Nrf2 pathway. *Nat Commun.* 2020;11:348. doi:[10.1038/s41467-019-14190-2](https://doi.org/10.1038/s41467-019-14190-2)
32. Zhou S, Peng J, Xiao L, et al. TRIM25 regulates oxaliplatin resistance in colorectal cancer by promoting EZH2 stability. *Cell Death Dis.* 2021;12:463. doi:[10.1038/s41419-021-03734-4](https://doi.org/10.1038/s41419-021-03734-4)

**How to cite this article:** Tang H, Li X, Jiang L, et al. RITA1 drives the growth of bladder cancer cells by recruiting TRIM25 to facilitate the proteasomal degradation of RBPJ. *Cancer Sci.* 2022;113:3071-3084. doi: [10.1111/cas.15459](https://doi.org/10.1111/cas.15459)

#### SUPPORTING INFORMATION

Additional supporting information can be found online in the Supporting Information section at the end of this article.